DOI: 10.1002/ejoc.200600765

Investigating Organization of Molecules that Facilitates Intermolecular Acyl Transfer in Crystals: Reactivity and X-ray Structures of *O*-Benzoyl-*myo*-inositol 1,3,5-Orthoesters

Chebrolu Murali,[a] Mysore S. Shashidhar,*[a] Rajesh G. Gonnade,[b] and Mohan M. Bhadbhade*[b]

Keywords: Inositol / Solid-state reaction / Transesterification / Weak interactions / Molecular self assembly

Crystal structure analysis of racemic 2,6-di-*O*-benzoyl-*myo*-inositol 1,3,5-orthobenzoate reveals helical organization of the molecules, remarkably similar to that observed earlier in crystals of racemic 2,6-di-*O*-benzoyl-*myo*-inositol 1,3,5-orthoformate. Both these dibenzoates are isostructural despite the bulkier phenyl substituent in place of hydrogen. The latter compound shows highly facile intermolecular benzoyl transfer reactivity in its crystals and as anticipated from the crystal structure, the orthobenzoate indeed exhibits facile benzoyl transfer reactivity in its crystals. 2-*O*-Benzoyl-*myo*-inositol 1,3,5-orthoformate and the corresponding orthobenzoate also undergo transesterification in their crystals, but the specificity of acyl transfer is very low, and the reaction yields a mixture of products. The parameters of helical molecular assembly that facilitates acyl transfer in crystals have been investigated. A comparison of the molecular assemblies and lattice interactions in crystals of all the four compounds with the observed reactivity patterns show that facile acyl transfer reaction is brought about by a modular "reaction tunnel" formed by helical pre-organization of molecules, favorable electrophile···nucleophile contacts and weak interactions that hold the acyl group in the "right" orientation for the attack by the nucleophile. Acyl transfer reaction in all the four derivatives was also carried out in solution for comparison.

Introduction

There is an upsurge in interest in the study of solvent free organic synthesis,[1] including the use of ionic liquids[2] and reactions in aqueous media,[3] due to environment related reasons. Among these methods, reactions in molecular solids are of interest from synthetic as well as mechanistic points of view.[1,4] Often reactions in crystals proceed with high facility, regio- and stereoselectivity due to topochemical control in molecular crystals, as compared to their solution state reactions.[4,5] Since determination of conformation, relative orientation and non-covalent interactions of reacting molecules with their neighbors in crystals is possible by X-ray diffraction analysis, analysis of the crystal structure of reactants could provide information on the mechanism and course of organic reactions in the solid-state. Only a few types of reactions occurring in crystals such as addition reactions to carbon–carbon multiple bonds,[6] carbon–carbon bond cleavage in carbonyl compounds,[7] certain radical forming reactions[8] have been studied in detail and these have provided great insight into the mechanism of these reactions. Such detailed studies on other types of reactions in molecular crystals have not been reported. However, there are reports on synthetically useful solid-state organic reactions[1] many of which have not been investigated systematically. Although, the topochemical criteria for double bond juxtaposition has been well recognized for the [2+2] dimerization or polymerization reactions in the crystalline state,[6] such detailed analysis for other types of reactions has not been carried out.

As a part of an ongoing program on the solid-state structure and chemical reactivity of inositol derivatives, we had earlier reported the facile transesterification reactions in molecular crystals[5] and co-crystals of *O*-benzoylated *myo*-inositol orthoformate derivatives.[9] We herein reveal our results on the transesterification reaction of *myo*-inositol orthoester derivatives **1**, **5** and **6** which are facilitated in the crystalline state as compared to the same reaction in solution. The crystal structure–reactivity correlations presented here support our earlier proposition[9] that helical molecular pre-organization with favorable weak intermolecular interactions in the crystal lattice aid these transesterification reactions.

[a] Division of Organic Synthesis, National Chemical Laboratory, Pune 411008, India
E-mail: ms.shashidhar@ncl.res.in
[b] Center for Materials Characterization, National Chemical Laboratory,
Pune 411008, India
Fax: +91-20-25902642
E-mail: mm.bhadbhade@ncl.res.in

Supporting information for this article is available on the WWW under http://www.eurjoc.org or from the author.

Results and Discussion

Benzoyl Transfer Reaction in Crystals

Crystals of the racemic orthobenzoate **1**, when heated with solid sodium carbonate undergo facile transesterification to give the tribenzoate **3** and the diol **5** in almost quantitative yield (Scheme 1 and Table 1). At lower temperatures, the reaction proceeds smoothly but the conversion is slower, as expected. The DSC curve of **1** consists of only a single endotherm (melting, see Supporting Information) and does not show any phase changes in the temperature range applied for reactions in the crystalline state. Interestingly, base-catalyzed transesterification of the same dibenzoate **1** in solution (at comparable temperature) is less facile and **1** does not react at all, at ambient temperature (25–30 °C). Reaction of the racemic dibenzoate **1** in the molten state affords a mixture of several products and was not as clean as the reaction in crystalline and solution states.

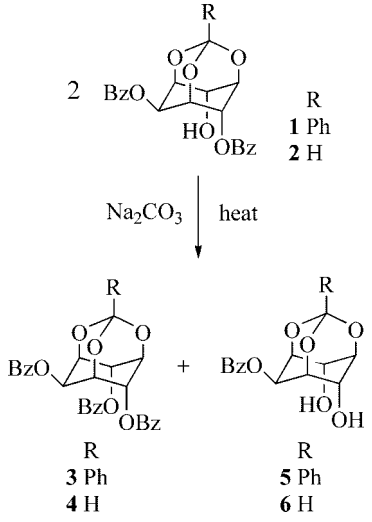

Scheme 1.

Table 1. Summary of results of transesterification of the benzoates **1** and **2** under different conditions.

Entry	Reactant	Solvent / base / temp. (°C) / time (h)	Yield (%)[a]
1	**1**	– / Na_2CO_3 / 140 / 62	**3** (49) **5** (48)
2	**1**	– / Na_2CO_3 / 120 / 62	**3** (33) **5** (32)
3[b]	**2**	– / Na_2CO_3 / 140 / 60	**4** (47) **6** (49)
4[b]	**2**	– / Na_2CO_3 / 120 / 60	**4** (31) **6** (30)
5	**1**	DMF / DIPEA[c] / 130 / 72	**3** (16) **5** (14)
6	**1**	DMF / DIPEA / r.t.[d] / 72	**3** (0) **5** (0)
7	**2**	DMF / DIPEA / 130 / 60	**4** (29) **6** (27)
8	**2**	DMF / DIPEA / r.t.[d] / 120	**4** (10) **6** (8)
9	**1**	–[e] / Na_2CO_3 / 120 / 60	–[f] –
10	**2**	–[e] / Na_2CO_3 / 120 / 60	–[f] –

[a] This reaction being a disproportionation reaction, the maximum yields possible for **3**–**6** is 50% each. [b] From ref.[5] [c] Diisopropylethylamine. [d] Ambient temperature. [e] Reaction in melt. [f] Mixture of several products was obtained; see experimental section for details.

A comparison of the results (Table 1) of transesterification shows that transesterification is equally facile in crystals of **1** and **2**[5] but not in solution. The reactivity of **1** in solution is less than that of **2**. These results strongly support the assumption of a significant role of the molecular packing in crystals on the benzoyl transfer reactivity of **1** and **2**.

Earlier[10] we reported on the NaH-assisted facile intermolecular acyl migration in racemic 4-*O*-acyl-*myo*-inositol 1,3,5-orthoesters **7** (Scheme 2) to give the corresponding 2-*O*-acyl derivatives **8** in excellent yields (>90%) in the solution state. The same reaction in solution is irreversible and the 2-*O*-acyl-*myo*-inositol 1,3,5-orthoesters **8** are completely stable both in the presence of strong bases (sodium hydride or potassium *tert*-butoxide) and at higher temperatures. Analysis of the crystal structures of the 2-benzoates **5** and **6** reveals the relative orientation of molecules that appears conducive for the solid-state acyl-transfer reactivity, in a fashion similar to crystals of racemic **1** and **2**. Hence we subjected crystals of the diols **5** and **6** to transesterification conditions in the presence of solid sodium carbonate. Although this reaction yields transesterified products, it is not a clean reaction. The various products obtained from **6** are shown in the Scheme 2. Transesterification of crystalline orthobenzoate **5** also yields a mixture of products similar to that observed in the case of the orthoformate **6**. It is interesting to note that although both these benzoates fail to undergo transesterification in solution, they undergo the same reaction in the crystalline state owing to the relatively "frozen" assembly of molecules favorable for the transesterification reaction. Facility and specificity of the transesterification in crystals of **5** and **6** are not as good as those in crystals of **1** and **2** due to differences in the packing of the molecules in their crystals as discussed in the next section.

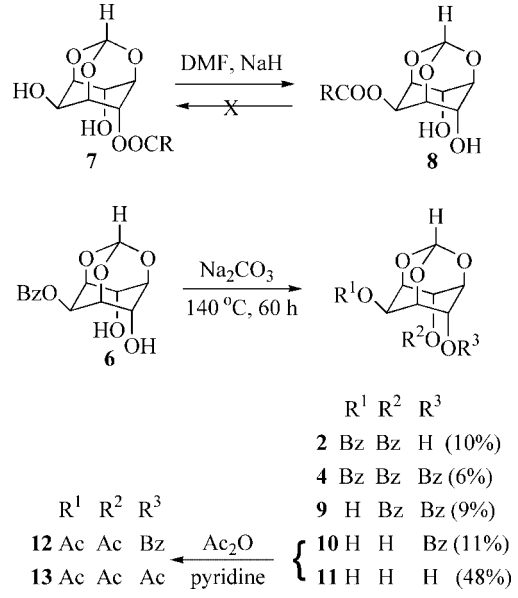

Scheme 2.

Correlation of Molecular Pre-Organization and Intermolecular Interactions with Acyl Transfer Reactivities

The crystal structure analyses of diester **1** and monoesters **5** and **6** were carried out with the aim to correlate their solid-state reactivities with crystal structures. Crystals of **1** and **6** belong to the monoclinic space groups $P2_1/c$ and $P2_1/n$ respectively, whereas **5** spontaneously resolved to yield chiral crystals (orthorhombic, space group $P2_12_12_1$) irrespective of the solvent used. Our attempts to obtain an achiral polymorph of **5** were not successful. Cases where the *meso* compounds like **5** produce optically active crystals are intriguing, having significance both in understanding the fundamental process of crystallization[11] as well as in their applications as NLO materials.

The molecules in crystals of **1** are arranged helically around a crystallographic twofold screw axis via O–H···O hydrogen bonding, very similar to the arrangement of molecules in crystals of the orthoformate derivative **2**.[9] The OH group at the C-4 position in **1** donates its H atom to the carbonyl oxygen O7 of the C2–*O*-acyl group forming a helical assembly along the *b*-axis. It is interesting to note that this helical architecture is retained (Figure 1, A and Table 2) even when the orthoformate H (in **2**[9]) is replaced by a phenyl group (as in **1**). This "reactive" helical pre-organization shows two striking geometrical similarities – first the electrophile (El)···nucleophile (Nu) interaction (Figure 1, B and Table 3) and secondly the C–H···π[12] interaction that the leaving benzoyl group makes with the C–H group of the reacting partner molecule along the helix (Figure 1, B and Table 2). Also, the O6–C15 bond length of the C6-axial benzoate group is longer [1.347(2) Å] compared to the chemically equivalent O2–C8 bond of the C2-equatorial benzoate group [1.334(2) Å], a feature noted in the reactive crystals of the orthoformate derivative **2**.[9] In fact, the El···Nu geometrical parameters are better in crystals of **1** (Table 3) than those observed in crystals of **2**.[5,9] The helices thus assembled (Figure 1, C) are thought to provide "reaction tunnels" throughout the crystal with the intermolecular benzoyl transfer going in a "domino" fashion within each helix.[9] It is also important to note the packing of individual helices in crystals (Figure 1, C). In crystals of **1**, they are linked to each other by C–H···O interactions between the C–H group of the inositol ring with carbonyl oxygen of the C6–*O*-benzoyl group. Additionally, the C–H group of C6–*O*-benzoyl group also makes C–H···O contact with ether oxygen of the C2–*O*-benzoyl group (see Supporting Information for details).

Table 2. Intermolecular hydrogen bonding and C–H···π interactions in crystals of **1**, **5** and **6**.[a]

	D–H···A	H···A [Å]	D···A [Å]	D–H···A [°]
1	O(4)–H(4A)···O(7)[b]	1.97(2)	2.795(2)	168(2)
	C(3)–H(3)···Cg(2)[c]	2.83	3.805	166
5	O(4)–H(4A)···O(3)[d]	2.56(3)	3.018(2)	117(2)
	O(6)–H(6A)···O(1)[b]	2.11(3)	2.861(2)	156(3)
	C(5)–H(5)···Cg(1)[d]	3.91	4.720	139
6	O(4)–H(4A)···O(1)[e]	1.90(3)	2.656(2)	159(3)
	O(6)–H(6A)···O(3)[f]	2.53(3)	3.063(3)	123(2)
	C(5)–H(5)···Cg(1)[e]	2.64	3.561	162

[a] Cg = ring centre-of-gravity (centroid), Cg1 = C9–C14, Cg2 = C16–C21. Symmetry codes: [b] $-x, -1/2 + y, 1/2 - z$. [c] $-x, 1/2 + y, 1/2 - z$. [d] $1 - x, -1/2 + y, 1/2 - z$. [e] $1/2 + x, 1/2 - y, -1/2 + z$. [f] $-1/2 + x, 1/2 - y, -1/2 + z$.

Table 3. Geometry of the reacting groups (El···Nu) in crystals of **1**, **5** and **6**.

Distance or angle	**1**	**5**	**6**
C15(C8)···O4	3.144(2) Å[a]	3.532(2) Å[b]	3.628(2) Å[c]
O4···C15(C8)–O8(O7)	85.6(1)°	106.1(2)°	105.6(2)°
C4–O4···C15(C8)	111.1(1)°	112.1(2)°	110.3(2)°
H4A–O4···C15(C8)	113(1)°	77(1)°	73(1)°

Symmetry codes: [a] $-x, -1/2 + y, 1/2 - z$. [b] $1 - x, 1/2 + y, 1/2 - z$. [c] $-1/2 + x, 1/2 - y, 1/2 + z$.

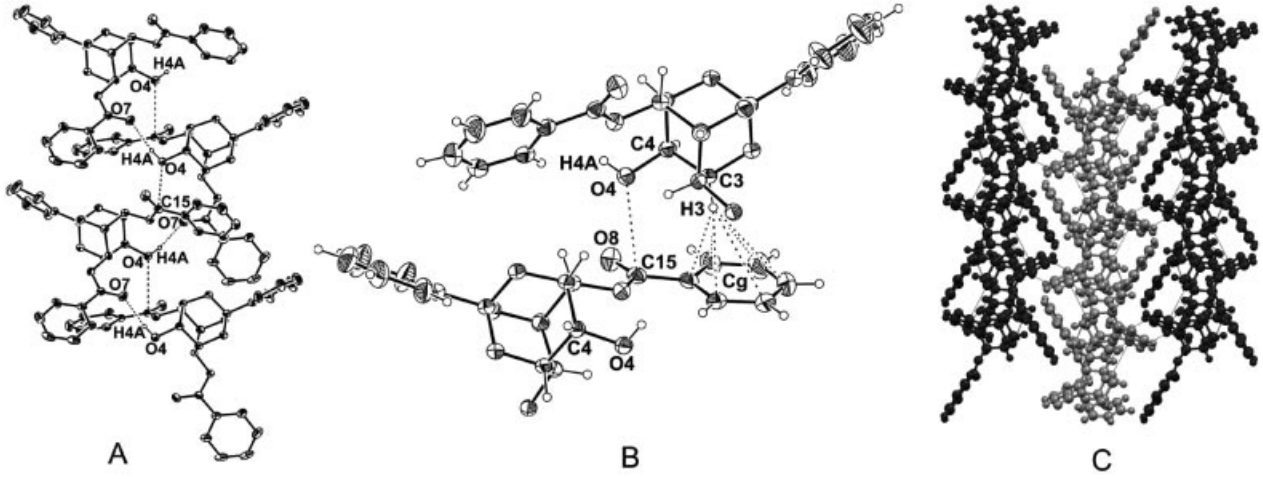

Figure 1. A) Helical self-assembly of **1** via O–H···O hydrogen bonding in its crystals, B) relative orientation of the reacting molecules in crystals of **1** (the 2-*O*-benzoyl group is not shown for clarity) and C) packing of helices in crystals of **1**.

Although the benzoates **5** and **6** have two hydroxy groups at C4 and C6 positions, these molecules do not assemble by forming intermolecular O–H···O hydrogen bond in their crystals, from either of these with the O=C of the C2-benzoate group. In both **5** and **6**, intermolecular O–H···O bonding is formed between the OH group at the C4 and C-6 position and the oxygen O1 and O3 of the orthoformate (Table 2). Intramolecular O–H···O bond exists with the C4–OH donating its proton to the oxygen of the C6–OH group in both **5** and **6**. Detailed molecular organization in crystals of **5** and **6** is described below.

The helical assembly in crystals of **5** is formed by the O4–H4A···O3 interaction around 2_1-screw axis (Figure 2, A). However, one can also imagine another helix that is formed via O6–H6A···O1 hydrogen bonding, again along the *b*-axis (Table 2). Actually, these two helices are part of an extended two-dimensional sheet created by crystallographic 2_1 screw axis along *b*-axis. The first helix brings the two reacting groups C2–*O*-benzoyl group (El) and the C4-hydroxy group (Nu) of the adjacent molecule closer along the helix axis (Figure 2, B), but the El···Nu distance [C8···O4 3.532(2) Å] is somewhat longer than that seen in crystals of **1** and **2**. However, the angle of approach of Nu to El (O4···C8–O7 106.1°, Table 3) is closer to the tetrahedral value. The phenyl ring of the C2–*O*-benzoyl group is not engaged with any C–H group of the inositol ring in the formation of C–H···π contacts (Table 2). The second helical assembly with O6–H6A···O1 interactions makes very long and unfavourable El ···Nu contacts (Table 4). Furthermore, the entire sheet structure (Figure 2, C) does not leave a "modular" reaction channel in the crystal lattice for the reaction to proceed in contrast to that observed in crystals of **1** (Figure 1).

In crystals of **6**, the one-dimensional assembly although appears to be "helical" (Figure 3, A), the molecules along the string are actually related by n-glide of the space group

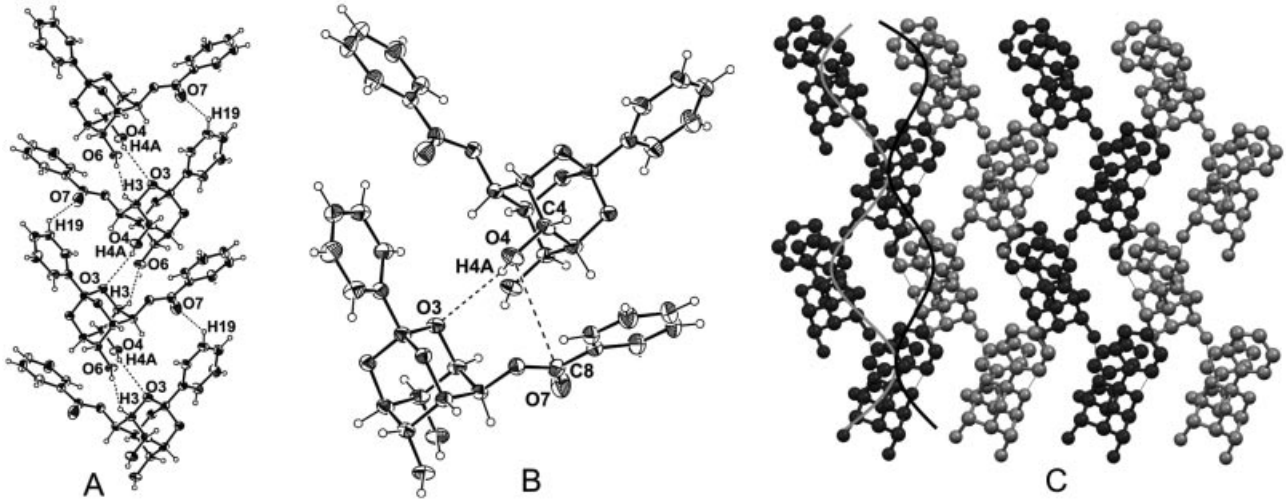

Figure 2. A) Helical self-assembly via O4–H4A···O3 hydrogen bonding in crystals of **5**, B) relative orientation of the reacting molecules in crystals of **5** and C) intersecting of helices (O4–H4A···O3, grey curved line and O6–H6A···O1, black curved line) forming two dimensional sheet in crystals of **5**.

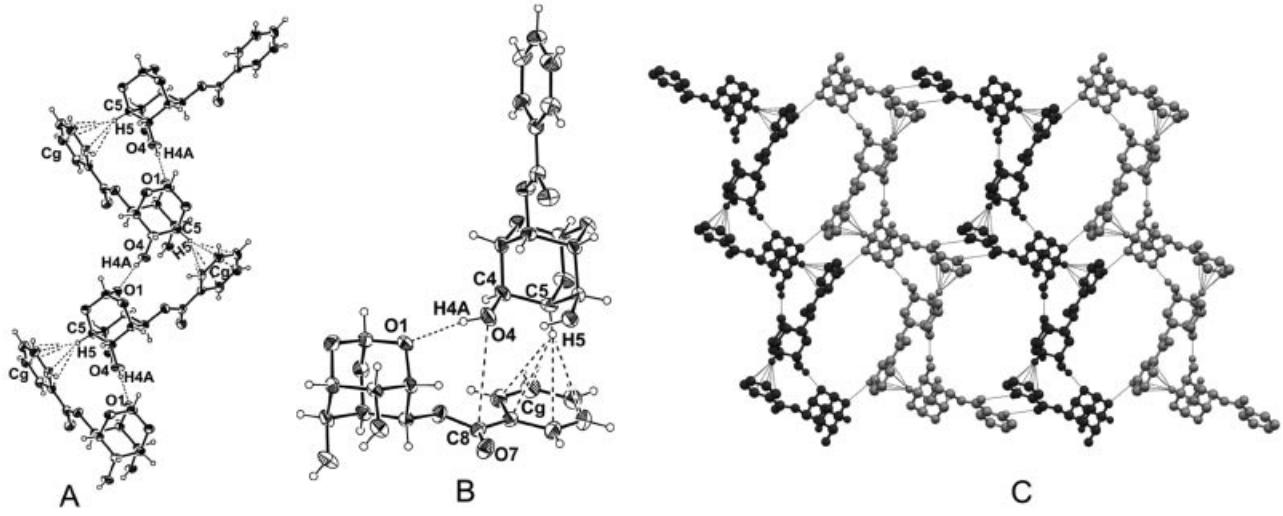

Figure 3. A) Association of molecules in crystals of **6** via O4–H4A···O1 hydrogen bonding interaction, B) relative orientation of the reacting molecules in crystals of **6** and C) linking of helices via C–H···O contact forming two dimensional sheet.

Table 4. Geometry of the reacting groups in crystals of **5** and **6** along 2_1-screw and diagonal glide related molecule respectively.

Distance or angle	**5**	**6**
C8···O6	4.599(3)[a], 4.128(3) Å[b]	4.452(3) Å[c]
O6···C8–O7	149.6(2), 64.9(2)°	154.2(2)°
C6–O6···C8	77.8(3), 109.2(3)°	140.3(2)°
H6A–O6···C8	48(1), 104(1)°	101(1)°

Symmetry codes: [a] $-x$, $-1/2 + y$, $1/2 - z$. [b] $1 - x$, $1/2 + y$, $1/2 - z$. [c] $-1/2 + x$, $1/2 - y$, $-1/2 + z$.

symmetry. The O4–H4A···O1 hydrogen bonded glide related molecules self-assemble to bring the electrophile and the nucleophile together (Figure 3, B) with an angle close to the tetrahedral value (angle O4···C8–O7 105.6°, Table 3) but again with somewhat longer El···Nu (C8···O4) distance (3.628 Å) as compared to crystals of **1** or **2**. However, the geometry of C–H···π contacts made by the C5–H5 of the inositol ring with the phenyl ring of the C2–*O*-benzoyl group from the next molecule is significantly better as compared to **1** (Table 2). The self-assembled (diagonal glide related) chains make centrosymmetric inter-chain contacts essentially of C–H···O type (Figure 3, C and Supporting Information for more details).

In addition to O4–H4A···O1 contact, the molecules of **6** also form another chain via O6–H6A···O3 bonding as well as via C14–H14···O6 contact (see Supporting Information) along the diagonal glide related molecules. But along this direction, the reactive groups C6–OH and C2–OBz are not at all in close proximity; the El···Nu distance is 4.452 Å (O6···C8) and angle O6···C8–O7 154.2° (Table 4). Further, there is no C–H···π interaction along these chains. These chains are linked with each other along b-axis by C–H···O contact between the C–H groups of the C2–*O*-benzoyl group and with one of the orthoformate oxygen (see Supporting Information for details). Unfavorable approach geometry of the Nu with respect to El and lack of a reaction channel (as in crystals of **1**) in crystals of **5** and **6** might well explain the low facility of the acyl transfer reaction in crystals of **5** and **6** as compared to the reactivity of **1** and **2** in their crystals.

Conclusions

A comparative study on the intermolecular acyl transfer reactivity of benzoates **1**, **2**, **5** and **6** in their crystals as well as in solution and an analysis of their crystal structures show that (a) acyl transfer reactivity in crystals is controlled by the relative geometry and juxtaposition of the hydroxy and ester groups; (b) weak intermolecular interactions[12] between the reacting molecules in the crystal lattice and (c) packing of molecules in crystals that provide "reaction channels" for the propagation of the reaction. A comparison of the reactivity of monobenzoates **5** and **6** in solution and crystals show that molecules that are un-reactive in solution can be coaxed to react in crystals due to proximity of the reacting groups and crystal packing parameters. The crystal structure reactivity correlation described for crystals of **1** is the third example that we have encountered in our laboratory (for first two examples see ref.[5,9]). Hence, this spontaneously assembled "reactive" molecular pre-organization in crystals of **1** promises to be valuable while designing reactive crystals that facilitate intermolecular acyl transfer reactions.

Experimental Section

Preparation of *rac*-2,6-Di-*O*-benzoyl-*myo*-inositol 1,3,5-Orthobenzoate (1): To a solution of *myo*-inositol 1,3,5-orthobenzoate[13] (2.130 g, 8.0 mmol) in dry pyridine (24 mL), freshly distilled benzoyl chloride (2.04 g, 17.6 mmol) was added dropwise over a period of 30 min at 0 °C. The reaction mixture was warmed up to room temperature and stirring was continued for 18 h. Solvents were removed under reduced pressure and the residue worked up with ethyl acetate. The crude product was chromatographed (eluent: ethyl acetate/dichloromethane/petroleum ether, 1:2:7) to get the tribenzoate **3** (0.385 g, 8%), racemic **1** (3.130 g, 82%) and **5** (0.095 g, 3%).

Data for 1: M.p. 187–189 °C. IR ($CHCl_3$): $\tilde{\nu}$ = 1722 (C=O), 3450–3620 (OH) cm^{-1}. ^1H NMR ($CDCl_3$, 200 MHz): δ = 2.60 (d, J = 5.8 Hz, 1 H, OH), 4.64–4.71 (m, 1 H, Ins H), 4.73–4.92 (m, 3 H, Ins H), 5.74 (t, J = 1.6 Hz, 1 H, Ins H), 5.92–6.02 (m, 1 H, Ins H), 7.35–7.53 (m, 7 H, Ar H), 7.53–7.66 (m, 2 H, Ar H), 7.66–7.80 (m, 2 H, Ar H), 8.03–8.22 (m, 4 H, PhCO *o*-H) ppm. ^{13}C NMR ($CDCl_3$, 50.32 MHz): δ = 63.0, 67.2, 68.5, 69.4, 71.0, 73.1 (Ins Cs), 107.7 ($PhCO_3$), 125.3, 128.1, 128.5, 128.6 (C_{arom}), 128.9 (C_{ipso}), 129.4 (C_{ipso}), 129.7, 129.8, 129.9, 133.5, 133.6 (C_{arom}), 136.6 (C_{ipso}), 165.3 (C=O), 166.3 (C=O) ppm. $C_{27}H_{22}O_8$ (474.47): calcd. C 68.35, H 4.67; found C 68.53, H 4.68.

Data for 3: M.p. 225–226 °C. IR ($CHCl_3$): $\tilde{\nu}$ = 1728 cm^{-1} (C=O) cm^{-1}. ^1H NMR ($CDCl_3$, 200 MHz): δ = 4.85–4.93 (m, 2 H, Ins H), 5.09–5.18 (m, 1 H, Ins H), 5.75–5.81 (t, J = 1.8 Hz, 1 H, Ins H), 5.95–6.05 (t, J = 4 Hz, 2 H, Ins H), 7.15–7.25 (m, 4 H, Ar H), 7.40–7.66 (m, 8 H, Ar H), 7.73–7.83 (m, 2 H, Ar H), 7.85–7.94 (m, 4 H, 2 PhCO *o*-H), 8.14–8.22 (m, 2 H, PhCO *o*-H) ppm. ^{13}C NMR ($CDCl_3$, 50.32 MHz): δ = 63.1, 67.8, 68.5, 70.8 (Ins Cs), 108.2 ($PhCO_3$), 125.5, 128.1, 128.4, 128.5 (C_{arom}), 129.4 (C_{ipso}), 129.9, 133.5 (C_{arom}), 136.4 (C_{ipso}), 165.2 (C=O), 166.2 (C=O) ppm. $C_{34}H_{26}O_9$ (578.57): calcd. C 70.58, H 4.53; found C 70.40, H 4.83.

Data for 5: M.p. 185–187 °C. IR (Nujol): $\tilde{\nu}$ = 1715 cm^{-1} (C=O), 3350–3600 (OH) cm^{-1}. ^1H NMR ($CDCl_3$, 200 MHz): δ = 4.00–4.10 (d, J = 4.8 Hz, 2 H, 2 OH), 4.45–4.56 (m, 1 H, Ins H), 4.61–4.70 (m, 2 H, Ins H), 4.73–4.85 (m, 2 H, Ins H), 5.64 (t, J = 1.8 Hz, 1 H, Ins H), 7.33–7.53 (m, 5 H, Ar H), 7.55–7.72 (m, 3 H, Ar H), 8.10–8.21 (m, 2 H, PhCO, *o*-H) ppm. ^{13}C NMR ([D_6]acetone, 50.32 MHz): δ = 64.0, 68.7, 70.9, 74.5(Ins Cs), 107.9 ($PhCO_3$), 126.5, 128.6, 129.5, 130.0, 130.5, 131.0 (C_{ipso}), 134.2, 138.9 (C_{ipso}), 166.4 (C=O) ppm. $C_{20}H_{18}O_7$ (370.36): calcd. C 64.86, H 4.89; found C 64.52, H 4.59.

Reaction of *rac*-2,6-Di-*O*-benzoyl-*myo*-inositol 1,3,5-Orthobenzoate (1) in the Solid State:[5] Crystals of **1** (0.119 g, 0.25 mmol) and sodium carbonate (0.213 g, 2.0 mmol) were ground together using mortar and pestle and heated in a sealed tube under argon atmosphere at 140 °C for 62 h. The reaction mixture was cooled to room temperature and extracted with chloroform/methanol mixture. The residue obtained from this extract was chromatographed to isolate **3** (0.071 g, 49%) and **5** (0.044 g, 48%).

Reaction of *rac*-2,6-Di-*O*-benzoyl-*myo*-inositol 1,3,5-Orthobenzoate (1) in the Molten State: Racemic **1** (0.119 g, 0.25 mmol) was melted and heated (190–195 °C) in a sealed tube under argon atmosphere

for 30 min. TLC analysis showed the presence of only the dibenzoate **1**. Finely powdered anhydrous sodium carbonate (0.213 g, 2 mmol) was then added and heating continued for 12 h. TLC analysis of the reaction mixture showed the presence of several products including **1**, **3**, **5** and *myo*-inositol 1,3,5-orthobenzoate. No attempt was made to separate these products.

Reaction of *rac*-2,6-Di-*O*-benzoyl-*myo*-inositol 1,3,5-Orthobenzoate (1) in Solution: A mixture of **1** (0.119 g, 0.25 mmol) and diisopropylethylamine (0.259 g, 2.0 mmol) in dry DMF (3 mL) was stirred at room temperature for 72 h. No reaction was observed. The same reaction when carried out at 130 °C for 72 h afforded the tribenzoate **3** (0.023 g, 16%) and the diol **5** (0.013 g, 14%) along with the unreacted **1** (68%).

Reaction of *rac*-2,6-Di-*O*-benzoyl-*myo*-inositol 1,3,5-Orthoformate[14] (2) in Solution: A mixture of **2** (0.2 g, 0.5 mmol) and diisopropylethylamine (0.519 g, 4 mmol) in dry DMF (3 mL) was stirred at room temperature for 120 h. (No products could be detected by TLC at the end of 60 h.) The solvents were removed under reduced pressure and the products were isolated by column chromatography (eluent: ethyl acetate/dichloromethane/petroleum ether, 1:1:8) to get **4** (0.025 g, 10%) and **6** (0.012 g, 8%) as white solids along with the unreacted starting material **2** (0.151 g, 76%).

Transesterification of 2-*O*-Benzoyl-*myo*-inositol 1,3,5-Orthobenzoate (5) in the Solid State: Crystals of **5** (0.185 g, 0.5 mmol) and sodium carbonate (0.424 g, 4.0 mmol) were ground together to give a fine powder and heated at 140 °C under argon atmosphere for 62 h. TLC analysis of the reaction mixture showed the presence of several products including **1**, **3**, **5** and *myo*-inositol 1,3,5-orthobenzoate. No attempt was made to separate these products.

Transesterification of 2-*O*-Benzoyl-*myo*-inositol 1,3,5-Orthoformate (6)[10] in the Solid State: Crystals of **6** (0.196 g, 0.66 mmol) and anhydrous sodium carbonate (0.565 g, 5.33 mmol) were ground together to a fine powder and heated at 140 °C under argon atmosphere for 60 h. The reaction mixture was cooled to room temperature and extracted with chloroform/methanol mixture (1:1, 2 × 10 mL). The residue obtained from this extract was chromatographed with 10% ethyl acetate in petroleum ether to get **2** (10%), m.p. 163–165 °C (ref.[14] m.p. 163–165 °C), **4** (6%), m.p. 215–217 °C (ref.[15] m.p. 216–218 °C), **9** (9%), m.p. 208–211 °C (ref.[16] m.p. 210–213 °C), **10** (11%), **11** (48%) and recovered starting material **6** (10%). Structures of **10** and **11** were established as their acetate derivatives **12** and **13**. To a mixture of **10** and **11** (0.086 g) in dry pyridine (2 mL), acetic anhydride (0.5 mL, 5.18 mmol) was added drop wise at 0 °C over a period of 30 min and the mixture was stirred for 8 h at room temperature. Solvents were removed under reduced pressure and the residue worked up with ethyl acetate. The crude product was chromatographed (eluent: 20% ethyl acetate in petroleum ether) to get **12** (0.028 g) and **13** (0.102 g), m.p. 172–174 °C (ref.[17] m.p. 173–174 °C). Data for **12**: m.p. 167–169 °C. IR ($CHCl_3$): $\tilde{\nu}$ = 1738 (C=O) cm^{-1}. ^1H NMR ($CDCl_3$, 200 MHz): δ = 1.79 (s, 3 H, CH_3), 2.24 (s, 3 H, CH_3), 4.35–4.43 (m, 1 H, Ins H), 4.45–4.52 (m, 1 H, Ins H), 4.68–4.78 (m, 1 H, Ins H), 5.33–5.40 (m, 1 H, HCO_3), 5.55–5.67 (m, 2 H, Ins H), 5.72–5.78 (m, 1 H, Ins H), 7.40–7.53 (m, 2 H, Ar H), 7.55–7.68 (m, 1 H, Ar H), 7.98–8.10 (m, 2 H, PhCO, *o*-H) ppm. ^{13}C NMR ($CDCl_3$, 50.32 MHz): δ = 20.3 (CH_3), 21.0 (CH_3), 63.2, 66.3, 67.5, 67.7, 69.0, 69.2 (Ins Cs), 103.0 (HCO_3), 128.6, 128.7, 129.7, 133.8, 164.7 (C=O), 169.0 (C=O), 170.5 (C=O) ppm. $C_{18}H_{18}O_9$ (378.33): calcd. C 57.15, H 4.79; found C 56.79, H 4.68.

Table 5. Summary of crystal data, data collection, structure solution and refinement details for **1**, **5** and **6**.

Crystal data	**1**	**5**	**6**
Formula	$C_{27}H_{22}O_8$	$C_{20}H_{18}O_7$	$C_{14}H_{14}O_7$
M_r	474.45	370.34	294.25
Crystal size, mm	0.38 × 0.33 × 0.28	0.41 × 0.15 × 0.13	0.51 × 0.23 × 0.22
Temp. [K]	297(2)	297(2)	297(2)
Crystal system	monoclinic	orthorhombic	monoclinic
Space group	$P2_1/c$	$P2_12_12_1$	$P2_1/n$
a [Å]	14.819(2)	6.2886(17)	6.198(3)
b [Å]	9.4652(14)	11.361(3)	17.764(10)
c [Å]	16.977(3)	23.481(6)	11.748(7)
β [°]	103.908(3)	90	91.599(14)
V [Å^3]	2311.5(6)	1677.6(8)	1293.0(13)
Z	4	4	4
F(000)	992	776	616
D calcd. [g cm^{-3}]	1.363	1.466	1.512
μ [mm^{-1}]	0.101	0.112	0.123
absorption correction	multi-scan	multi-scan	multi-scan
T_{min}	0.9628	0.9552	0.9400
T_{max}	0.9726	0.9851	0.9733
Reflections collected	11265	12068	6204
Unique reflections	4053	2963	2263
Observed reflections	3254	2498	1989
Index range	–16⇒h⇒17, –9⇒k⇒11, –15⇒l⇒ 20	–7⇒h⇒7, –13⇒k⇒8, –27⇒l⇒ 26	–5⇒h⇒7, –21⇒k⇒19, –7⇒l⇒ 13
R_1 [$I > 2\sigma(I)$]	0.0384	0.0396	0.0464
wR_2	0.0953	0.0757	0.1071
R_1 (all data)	0.0509	0.0501	0.0539
WR_2 (all data)	0.1032	0.0788	0.1110
Goodness-of-fit	1.037	1.048	1.128
$\Delta\rho_{max}$,$\Delta\rho_{min}$ [e Å^{-3}]	–0.174, 0.157	–0.126, 0.143	–0.173, 0.153
CCDC number	617709	617710	617711

X-ray Crystal Structure Determinations: Single crystals of the diester **1** and the monoesters **5** and **6** were obtained from chloroform and light petroleum mixture and good quality crystals were selected using Leica Polarizing microscope. X-ray intensity data were collected on a Bruker SMART APEX CCD diffractometer with omega and phi scan mode, λ_{Mo}-K_α = 0.71073 Å at T = 297(2) K. All the data were corrected for Lorentzian, polarization and absorption effects using Bruker's SAINT and SADABS programs. SHELX-97[18] was used for structure solution and full-matrix least-squares refinement on F^2. Hydrogen atoms of the inositol ring and hydroxy group of **1** were located in the difference Fourier map and the rest were included in the refinement as per the riding model, whereas for **5**, all the H-atoms were located in the difference Fourier map and refined isotropically. Crystal data and details of data collection, structure solution and refinements for **1**, **5** and **6** are summarized in Table 5. All the weak interaction calculations were carried out using PLATON.[19]

CCDC-617709 to -617711 contain the supplementary crystallographic data for this paper. These data can be obtained free of charge from The Cambridge Crystallographic Data Centre via www.ccdc.cam.ac.uk/data_request/cif.

Supporting Information (for details see also the footnote on the first page of this article): i) Table for weak intermolecular interactions in crystals of **1**, **5** and **6** (other than those given in Table 2). ii) colour version of the Figures 1, 2 and 3. iii) DSC profile of compound **1**. iv) Packing of helices in crystals of **1**, **5** and **6**.

Acknowledgments

C. M. is recipient of a Senior Research Fellowship from CSIR, New Delhi, India. The valuable help by Dr. Smita Mule in recording the DSC runs is gratefully acknowledged. This work was supported by Department of Science and Technology, New Delhi.

[1] K. Tanaka, F. Toda, *Chem. Rev.* **2000**, *100*, 1025–1074.
[2] a) P. Wasserscheid, W. Keim, *Angew. Chem. Int. Ed.* **2000**, *39*, 3772–3789; b) T. Welton, *Chem. Rev.* **1999**, *99*, 2071–2084; c) A. R. Gholap, K. Venkatesan, R. Pasricha, T. Daniel, R. J. Lahoti, K. V. Srinivasan, *J. Org. Chem.* **2005**, *70*, 4869–4872.
[3] a) C.-J. Li, L. Chen, *Chem. Soc. Rev.* **2006**, *35*, 68–82; b) S. Kobayashi, K. Manabe, *Acc. Chem. Res.* **2002**, *35*, 209–217; c) U. M. Lindström, *Chem. Rev.* **2002**, *102*, 2751–2772.
[4] a) Y. Ohashi, K. Yanagi, T. Kurihara, Y. Sasada, Y. Ohgo, *J. Am. Chem. Soc.* **1982**, *104*, 6353–6359; b) J. H. Kim, S. M. Hubig, S. V. Lindeman, J. K. Kochi, *J. Am. Chem. Soc.* **2001**, *123*, 87–95; c) M. A. Garcia-Garibay, *Acc. Chem. Res.* **2003**, *36*, 491–498; d) D. Braga, F. Grepioni, *Angew. Chem. Int. Ed.* **2004**, *43*, 4002–4011.
[5] T. Praveen, U. Samanta, T. Das, M. S. Shashidhar, P. Charkrabarti, *J. Am. Chem. Soc.* **1998**, *120*, 3842–3845 and references cited therein.
[6] a) M. D. Cohen, G. M. J. Schmidt, *J. Chem. Soc.* **1964**, 1996–2000; b) M. D. Cohen, G. M. J. Schmidt, F. I. Sonntag, *J. Chem. Soc.* **1964**, 2000–2014; c) G. M. J. Schmidt, *J. Chem. Soc.* **1964**, 2014–2021.
[7] a) E. Cheung, M. R. Netherton, J. R. Scheffer, J. Trotter, *Org. Lett.* **2000**, *2*, 77–80; b) D. Braga, S. Chen, H. Filson, L. Maini, M. R. Netherton, B. O. Patrick, J. R. Scheffer, C. Scott, W. Xia, *J. Am. Chem. Soc.* **2004**, *126*, 3511–3520.
[8] V. Ramamurthy, K. Venkatesan, *Chem. Rev.* **1987**, *87*, 433–481.
[9] M. P. Sarmah, R. G. Gonnade, M. S. Shashidhar, M. M. Bhadbhade, *Chem. Eur. J.* **2005**, *11*, 2103–2110.
[10] K. M. Sureshan, M. S. Shashidhar, *Tetrahedron Lett.* **2000**, *41*, 4185–4188.
[11] R. G. Gonnade, M. M. Bhadbhade, M. S. Shashidhar, *Chem. Commun.* **2004**, 2530–2531.
[12] a) M. Nishio, M. Hirota, Y. Umezawa, *The CH/π Interaction: Evidence, Nature and Consequences*, Wiley-VCH, **1998**; b) R. Boese, T. Clark, A. Gavezzotti, *Helv. Chim. Acta* **2003**, *86*, 1085–1100; c) M. Nishio, *CrystEngComm* **2004**, *6*, 130–158.
[13] G. Bhosekar, C. Murali, R. G. Gonnade, M. S. Shashidhar, M. M. Bhadbhade, *Cryst. Growth Des.* **2005**, *5*, 1977–1982.
[14] T. Benarjee, M. S. Shashidhar, *Tetrahedron Lett.* **1994**, *43*, 8053–8056.
[15] T. Das, M. S. Shashidhar, *Carbohydr. Res.* **1997**, *297*, 243–249.
[16] T. Das, M. S. Shashidhar, *Carbohydr. Res.* **1998**, *308*, 165–168.
[17] H. W. Lee, Y. Kishi, *J. Org. Chem.* **1985**, *50*, 4402–4404.
[18] G. M. Sheldrick, SHELX97, Program for crystal structure solution and refinement, University of Göttingen (Germany), **1997**.
[19] A. L. Spek, PLATON, Bijvoet Centre for Biomedical Research, Vakgroep Kristal & Structuurchemie, University of Utrecht (The Netherlands), **1990**.

Received: September 1, 2006
Published Online: January 8, 2007

